Experimental and statistical investigation of drying effects on coated offset paper quality

PASI RAJALA AND TIMO M. KOSKINEN

ABSTRACT: The objective of the present investigation was to model and explain the mechanisms governing development of coated paper quality during the drying process. We paid specific attention to the mottling tendency of papers for offset printing. Studies for this investigation were carried out in two phases. In the first phase, a series of coating trials were run at two pilot coaters, where papers were coated and dried under a number of different conditions. In the second phase, paper samples were printed under controlled conditions to assess print quality. From the results and a simulation model, we determined the migration of water in the coating and the evaporation and water absorption rates into the base paper. Statistical analysis was used to identify the effect of drying conditions on final product properties. Drying conditions affected paper gloss, smoothness, density, and print mottle. Under our trial conditions, the drainage at 70% coating solids and the evaporation rate at 77% solids were the most significant drying factors correlating with paper final properties. We also noticed that a high web temperature in the early stages of drying increased paper roughness and decreased paper gloss. According to the results from our drying model, water movement into blade-coated lightweight coated base paper is dominated by diffusion when the temperature is moderate or high. Capillary flow is restricted to the surface of the base paper. When the coating color contains only latex as the binder, mottle is caused by uneven coating structure formation in the in-plane direction, probably resulting from uneven shrinkage of the adjacent coating. Variations in mottle are larger when a coating color contains starch as a water-soluble binder. Uneven binder concentration caused by uneven binder migration increases mottle tendency.

Application: This study shows that mottle tendency and roughness of wood-containing papers can be controlled by optimizing the drying of coating and by proper selection of the most influential coating raw materials.

Drying can significantly affect the quality of coated papers. Over the past 30 years, many studies have evaluated the effects of drying rate on the quality of offset papers. In the consolidation phase of the coating color, which begins at the first critical concentration (FCC) of the coating solids, the volume fraction of the solid phase becomes so high that the pigment and latex particles begin to touch each other. A meniscus will form in the pores, which are emptied of water. Capillary forces will start to shrink the coating because they are now bigger than the stabilizing electrostatic repulsion forces. When the pores continue to empty, with solids in the second critical concentration (SCC), the latex particles have lost their form and the coating structure has been formed [1]. After SCC, no further migration of material or change in coating structure occurs. The drying rate during the so-called "critical drying phase" is claimed to be the main factor causing mottle, i.e., unevenness of a pictured image in offset printing [2-4].

Uneven binder migration has been assumed to be the cause for uneven surface properties and print. Graab's tests [2] showed that initial drying can be effective without harming paper quality, but the drying rate must be low just before reaching critical solids of the coating, which is just before the evaporation rate begins to fall. This was the first study to show that the evaporation rate at consolidation is a critical parameter, yet evaporation rates were low (<20 kg/m^{2}h) and drying times long (1.2-2.0 seconds before consolidation) [2]. Engström et al. [5] have shown that there is a clear difference between starch- and latex-containing coating colors when it comes to the correlation between drainage of coating in the continuous phase and evaporation rate and their respective effect on mottle. Starch readily migrates, especially at high evaporation rates, while CMC/latex is generally known to migrate less. Even if binder migration with starch occurred because of high evaporation, latex did not migrate at all. Also very high evaporation rates (150 kg/m^{2}h) could be used at consolidation without causing mottle if delay before convective drying was short (90 milliseconds) [6]. This was valid both with starch containing and latex based colors. So far, no conclusive correlation between uneven binder migration and mottle has been found by direct analysis of surface binder content [5-8]. There have also been studies in which binder migration has been modeled, and simulations have been made, with binder diffusion rate and evaporation rate as variables. The simulations showed that fast initial drying limits binder deposition on the coating surface [9].

Uneven mass distribution of coating caused by fiber roughening of the base stock has been assumed to be the cause for uneven surface properties and print. The increase in the surface roughness of the base paper can redistribute the mass of the wet coating layer during the consolidation process. The coating layer will stretch and thin to cover a larger area as base paper roughness increases. [10].

Fundamental studies of the basic mechanisms taking place during the drying of coated papers have shed light on possible coating consolidation

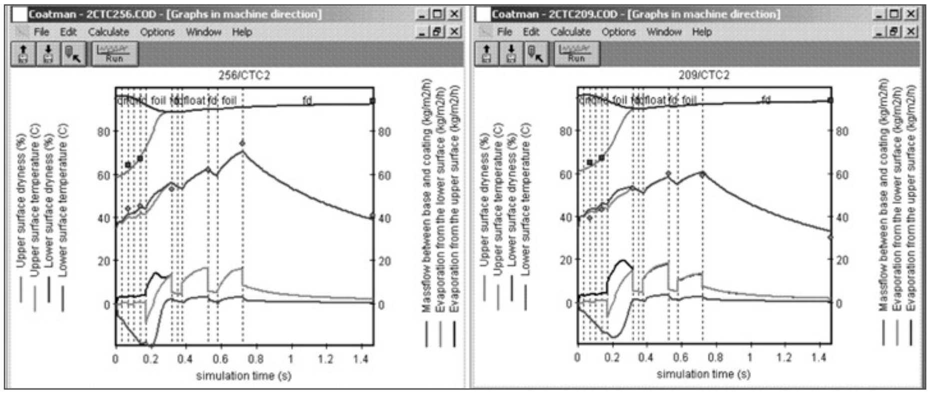

1. Simulation model output window of two interesting trial points.

Color	1	2	3	4	5
Clay, ND 3075	—	100	—	—	100
$CaCO_3$ Hydrocarb 90	—	—	50	—	—
Fine clay, Hydragloss 90	—	—	50	—	—
Delaminated US clay, Nugloss	—	—	—	100	—
Clay, SPS	100	—	—	—	—
SB latex Styronal FD 460	6	—	—	—	—
Styronal 805	—	11	11	11	9
Oxidized Starch, Raisamyl 302 E	6	—	—	—	3
CMC FF-30	1.5	0.3	0.3	0.3	0
Solids	59.0	58.1	61.5	60.1	59.2
ÅAGWR (0.5 bar, 120 s)	N/A	86	134	107	50

I. Coating color formulations used in the trials. Color 1 was used in trial CTC1, colors 2, 3, 4, and 5 in trial CTC2 and Color 4 in JAR2 trial.

mechanisms [1, 11-13]. Such studies suggest that chemical interactions between different coating components, together with drying, are responsible for the formation of the final coating layer structure [13].

Fiber swelling can cause irreversible changes in the base paper structure when water or coating color is applied onto paper [14, 15]. However, in the case of lightweight coated (LWC) paper, these changes are small or non-existent after the blade. Skowronski and Lepoutre [14] found that with high water absorption papers, swelling occurs before the blade, but with low water absorption papers, swelling occurs after the blade. The assumption we make here is that LWC papers are high water absorption papers. In addition, the above observations are valid for longer duration applicators (i.e., blade coater with an applicator roll or jet-applicator). In short-dwell time applicators, post- swelling is prevalent.

In spite of several interesting findings, no general theory about coating structure and paper quality development exists. When paper drying is studied, independent variables of interest are coating and dryer condition variables. Critical drying process variables are air temperature and velocity in air dryers and power input to infrared (IR) dryers. It is difficult to compare results from different pilot coaters with variable layouts. Formation of the coating layer structure depends on coat weight (CW) and air dryer and IR dryer powers, and other variables, such as the delay from coating application until the beginning of drying. Additionally, machine line speeds and coat weights often differ. Because of these reasons, we decided to construct a drying model and a simulation program to make comparisons easier, irrespective of coater layout.

DRYING MODEL

Our drying model is based on material and energy balance for an infinitesimal element of paper. The model describes mass and heat transfer in macroscopic, homogeneous material. Material properties of coating and paper are calculated from the properties of the constituent components according to their proportional weight [16]. We assumed that: (a) heat and mass transfer is one dimensional, (b) coating and base sheet are macroscopically homogenous, and (c) gravity, inertia, and deformation are negligible. The coefficients of the coupled differential equations are determined for both the coating layer and the base paper. Differential equations are solved numerically using the explicit forward finite difference method. The most important equations used are described briefly in Appendix A and in more detail in papers by Farkas and Karlsson [16, 17].

We define the key terminology as follows:

- *Evaporation rate* is the amount of water evaporated from the coated side of paper in a given time in a given area (kg/m^2h).
- *Drainage rate* is the amount of water transferred from the coating to the base stock, in a given time in a given area (kg/m^2h).
- *Average solids* is the solids content of coating, which is either calculated in the drying model, or measured in the laboratory from a scraped coating sample.
- *Falling rate* is the evaporation rate after constant evaporation rate, when the resistance of water movement inside the paper has begun to restrict the space of evaporation.
- *Delay time* is the period after the coating stage until a certain phase of drying is reached in the drying section, calculated by dividing the machine speed by the length in question in machine direction.

We verified the validity of the simulation program for the drying of coated paper by using results from several pilot coater trials. An important physical phenomenon—drainage—was determined in the model by calculating permeability for capillary flow and vapor diffusion resistance coefficients in Eq.s 2 and 5 in Appendix A, using data from tests with ÅA-GWR (Åbo Akademi gravimetrical water retention, Gradek, Finland). These values were then verified with pilot coater trials by scraping off the coating color and measuring the amount of drained water as a function of time and web temperature, as described by Heikkilä [18]. The drainage curve fit fairly well fitted when we assumed the water flow permeability parameter in Eq. 1 (Appendix A) was almost zero [19]. Åkerholm also verified the minor importance of capillary flow in coated paper drying through laboratory experiments [20].

We assume that, after application and leveling, drainage from viscous clay-based coating colors to porous LWC base stock takes place through diffusion. The amount of drained water before leveling is low; only about 0.5 g/m^2, which is equivalent to a 0.5 µm thick water layer, so there can not be much capillary continuity to base stock with large pores. Binder migration to base stock is then of minor importance. Water is partially evaporated from the filter cake-base stock boundary, condensed in the base paper, and partially diffused through the base paper [6]. Binder concentration can still be high in the top layer of the base paper and in the coating layer closest to the base paper. This does not exclude the possibility that binder can migrate to the base paper when coat weights are high, when coating color has low solids, when it does not form a dense filter cake, and when the base paper has a very fine capillary structure.

We ran simulations with two different coating recipes: 100% clay, 9 parts latex, and 3 parts starch containing Color 5 for the first, and 50% $CaCO_3$, 50% clay, 11 parts latex, and 0.3 parts CMC containing Color 3 for the second. We found substantial variation between the two coating colors with respect to how easily the coating layer dried. This was reflected in web temperatures. Falling rate drying starts when the coating surface is partly dry and the flow of water to the surface is not fast enough to keep evaporation at the maximum. The surface temperature then increases because of constant heat flow. The higher the web temperature needed to keep a sufficient drying rate during the falling evaporation rate drying stage, the higher the diffusion resistance of the coating color after SCC, the second critical concentration of coating during drying, as defined by Watanabe and Lepoutre [1]. **Figure 1** illustrates the model's presentation of this data.

Trial	Base	Color	Speed, m/min	Coating method	CW, g/m^2	Delay time before air drying, ms	Number of trial points
CTC1	PGW+BK	1	1000	Roll+blade	9	345	36
CTC2	PGW+BK	2-5	1800	SDTA+ blade	8-12	190	41
JAR2	TMP+BK	4	1400	Jet+blade	8-10	430	30

II. Coating methods, SB refers to surface blade and SD to short dwell.

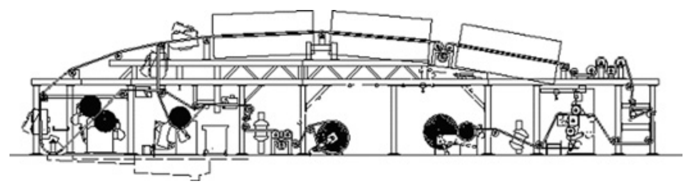

2. The lay-out of the CTC pilot coater.

Gloss CTC2		**Smoothness CTC2**	
Intercept	57.3	Intercept	1.08
Color	0.065	CW	-0.05
CW	1.574	Web temp.after IR	0.01
Web temp.after IR	-0.179		
Multiple R	0.90	Multiple R	0.83
R Square	0.81	R Square	0.69
Density CTC2		**Mottle CTC2**	
Intercept	986	Intercept	26.1
CW	21.03	CW	-0.86
Web temp.after IR	-1.22	2nd air dryer v, m/s	0.10
abs. 70% kg/m^2/h	4.52	abs. 70% kg/m 2/h	-1.40
Multiple R	0.90	Multiple R	0.85
R Square	0.81	R Square	0.72
Mottle CTC1		**Mottle, JAR 2**	
Intercept	27.6	Intercept	1.27
abs. 70% kg/m^2/h	-4.60	PM	0.276
evap.77% kg/m^2/h	0.50	IR 2 power, kW	-0.002
		abs70% kg/m^2/h	0.053
		evap.77% kg/m^2/h	-0.023
Multiple R	0.72	Multiple R	0.81
R Square	0.52	R Square	0.66

III. A selection of obtained regression models.

EXPERIMENTAL

Drying trials were run on two different pilot coaters to obtain sufficient data for the analysis of drying parameters on coated paper. A series of pilot coater trials were carried out at the CTC (Coating Technology Center, Raisio, Finland) and Valmet (Metso Corp.), Järvenpää, Finland, pilot facilities. In these tests, coated paper was dried by varying the relative amounts of infrared and airfoil drying, thereby obtaining a wide range of drying conditions. The simulation model was verified by the measurements made during the trials; the measured process parameters in the experiments were the air temperatures and jet exit air velocities. To measure air temperature, thermocouples were inserted into the air dryer nozzles. The outlet impingement air velocity from the nozzles was calculated from the static pressure in the air dryer nozzles. The web temperatures were recorded using an infrared pyrometer.

After supercalendering, the samples were printed on a 4-color, sheet-fed offset and heatset printing press at KCL (OY Keskuslaboratorio AB, Espoo, Finland). Mottle on the printed surface was determined by image analysis. The properties of the base paper and the printed paper were examined and the results were evaluated using the developed drying model. This was made by running simulation calculations after each trial.

The pigments used in the coating colors were English clay (SPS and ND 3075, English China Clay Int., UK) American clay (Nugloss, Engelhard Corporation, USA), fine clay (Hydragloss 90, J.M. Huber Corporation, USA), ground $CaCO_3$ (HC90, Omya Oy, Finland), CMC FF-30 (Metsä-Serla Chemicals OY, Finland), latex (Styronal 460 and 805, BASF GmbH, Germany), and starch (Raisamyl 302 E, Raisio Chemicals Oy, Finland). A gravimetric water retention method (ÅA-GWR, Gradek, Finland) was used to determine the dewatering rates of the coating colors using the TAPPI Standard Method. **Table I** shows the coating formulations.

The coating speed in trial CTC1 was 1000 meters per minute using a rigid blade and roll applicator set up. The coat weight was adjusted by tube pressure. The basis weight of the base paper was 40 g/m^2, the target moisture was 3.5% after the first pass and 5.5% after the second pass. In trial 2, the machine speed was 1800 m/min and the application method was SDTA,

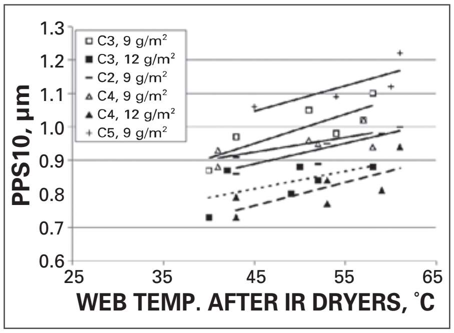

3. PPS-roughness vs. sheet surface temperature after IR dryers.

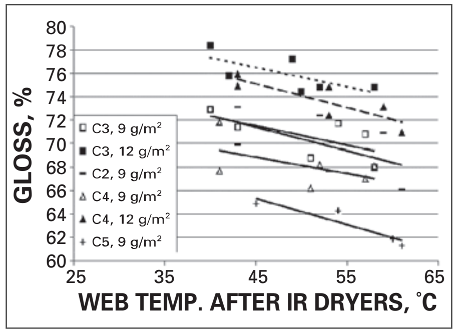

4. Gloss vs. sheet surface temperature after IR dryers

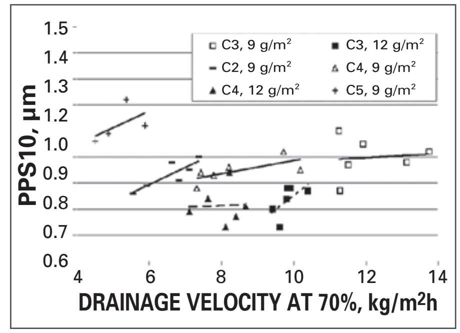

5. PPS-roughness vs. drainage at 70% solids. (Drainage was calculated using the simulation model).

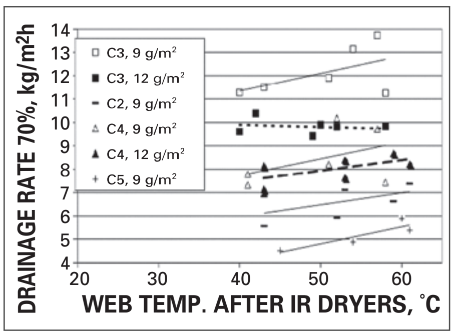

6. Drainage at 70% solids vs. web temperature after IR dryers

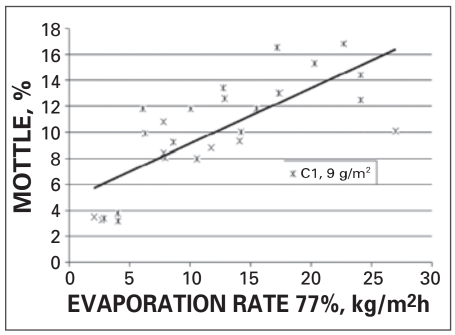

7. Mottle vs. evaporation rate at 77% solids when binder composition was starch 6% and latex 6%, delay to air drying 340 ms.

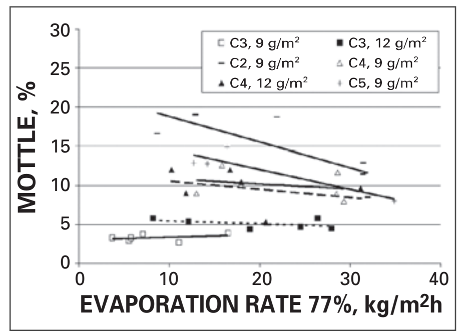

8. Mottle vs. evaporation rate at 77% solids with latex binder, while C5 contains also 3% starch, delay to air drying 190 ms.

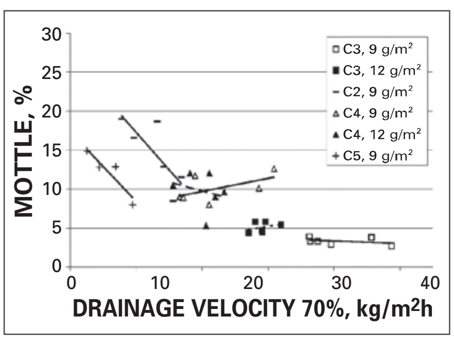

9. Mottle vs. drainage rate at 70% solids.

and in trial 3 machine, the speed was 1400 m/min and a jet applicator was used. **Table II** shows the target coat weights.

Controlled drying of the coating layer was primarily established by setting the infrared dryers to either 100%, 50%, or 15% of full power (460 kW/m, 230 kW/m, or 45 kW/m), with the co-radiators set at 80% (100 kW). The hot air dryers were then adjusted to different temperature levels (150˚C, 200˚C, and 250˚C) and air velocity levels (0-50 m/s, end moisture controll by velocity in the last dryer). **Figure 2** shows the layout of the pilot coater.

From previous studies, we expected that drying affects paper quality the most when the solids content of a coating is near its consolidated solids content [2-4]. From drying simulations, we collected data on evaporation and drainage rates and delay times when the solids content of the coatings were 70%, 75%, 77%, 80%, and 85%. The procedure was repeated for each trial condition. The paper qualities that were first tested in the correlation matrix were mottle (KCL- method); gloss (Hunter 75˚ gloss); roughness: PPS-10 (Parker Print-surf with a clamp pressure of 10 kpf/cm²), as in SCAN-P 21:67; density; IGT surface strength; opacity; and brightness.

From the correlation matrix, we found that drainage rate at 70% solids content and evaporation rate at 77% solids content correlated best with paper quality parameters. Therefore, we selected these values for further investigation. Using simulated results and the results of paper quality analysis, we developed linear regression models using the minimum square sum method (**Table III**). We calculated regression models stepwise. First, all drying variables were taken into the model. The least affecting variable was always rejected until all variables in the model were within confidence limits of 95%.

RESULTS AND DISCUSSION

Roughness, gloss, and density of paper

Increased web temperature at the beginning of the drying section increased roughness and decreased paper gloss (**Figs. 3** and **4**). Four different coating colors and two coat weights all behaved in a similar way. There could be several explanations for the roughening. Fiber rising in the base stock when it gets wet is a typical explanation for this kind of a phenomenon. Mechanical pulp fibers swell back close to the same thickness they had before machine-calendering of base paper.

Because drainage velocity into the base stock did not correlate with increased roughness, the explanation may not be that simple. **Figure 5** shows that temperature does not affect roughness by increasing drainage. Papers that are coated with low water retention coating colors had a similar roughness level and temperature affects in the same way as with other colors, even if the amount of drained water is bigger. We believe that the increased temperature of the base stock surface, wetted during the application and leveling stages of the coating, has an affect on the fibers causing relaxation and roughening.

Figure 6 shows that, although temperature has a positive correlation with the drainage rate, it is only one factor that contributes to drainage, and that coating color formulation is more important. In the JAR 2 trials, the delay time until the beginning of air drying, 430 ms, was so long that the effect of drying on any other paper properties, except mottle, was evened out. Heating the web with IR dryers and leaving it to condition in the free draw over a long enough period caused maximum relaxation of fibers.

Mottle

With starch containing coating color, the mottle tendency correlated well with the evaporation rate at 77 % solids (**Fig. 7**). This was also observed in a study by Norrdahl [4]. Delay time before air drying was 345 ms in these trials. However, coating colors containing no starch did show negative correlation between mottle and evaporation rate (**Fig. 8**), when the delay time before air drying was clearly shorter (190 ms). A higher evaporation rate even seemed to decrease the mottle, although the result was not statistically significant. Pigment type seems to be the key factor affecting mottle. Samples with starch showed approximately the same mottle level as those without starch. Uneven binder migration of soluble binder seems not to be the basic or main reason for mottle, although this is a common belief. It is more likely that uneven coating structure, which is probably caused by uneven shrinkage, created porosity variations in the coating in the in-plane direction, which then caused mottle [21]. Migration of starch probably intensifies this phenomenon.

When the water retention of the coating color was high, drainage rate at the beginning of drying, e.g., 70% average solids, reduced mottle (**Fig. 9**). With coating colors that have good water retention, increasing the web temperature in order to increase drainage, creates a porous coating. This, in turn, makes it possible to achieve a uniform porosity distribution in the in-plane direction of the coating.

Affect of uneven mass distribution

Because the mass distribution of coating in the in-plane direction of LWC paper varies a lot, there is typically a long distance between the coater blade and the dryer where the coating color reaches consolidation [22]. At solids of SCC, the final coating structure has been formed [1]. After this consolidation stage, drying has not been found to affect the quality of coated paper. The critical drying phase seems to be when the very surface of the paper coating layer with the highest coat weights (valleys) reaches its final structure. **Figures 10** and **11** illustrate that, on an average LWC coating, consolidation takes place during a relatively long period at the drying section. The coat weight of 3 g/m^2 is consolidated in the first free draw after the blade, but the consolidation of 15 g/m^2 does not take place until the second air dryer. The critical stage for paper quality is in the first air dryer, where coat weights of 12 g/m^2 are consolidated. The optimal drying strategy for this trial set was to target a relatively moderate drying rate in the first air dryer. However, we can not conclude that the whole coating layer has to be consolidated under moderate conditions. Rather, some specific parts of the coating (the valleys) have to be consolidated under these moderate conditions. The reason is that the thinner parts of the

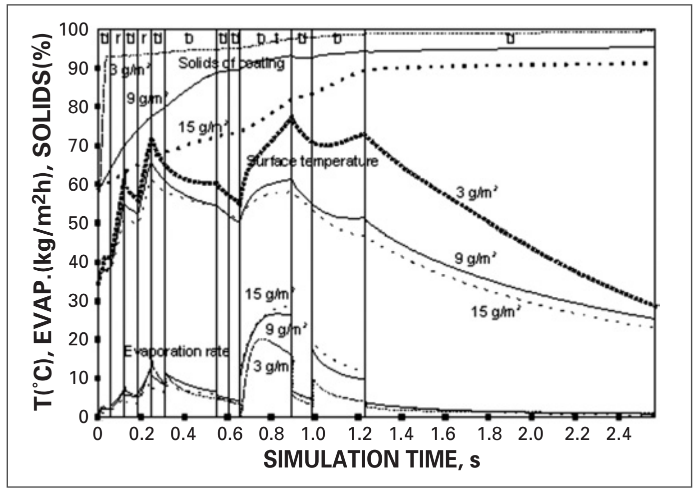

10. Simulation of the consolidation of 3, 9, and 15 g/m^2 coating. Average CW is 9 g/m^2, first dryer is open.

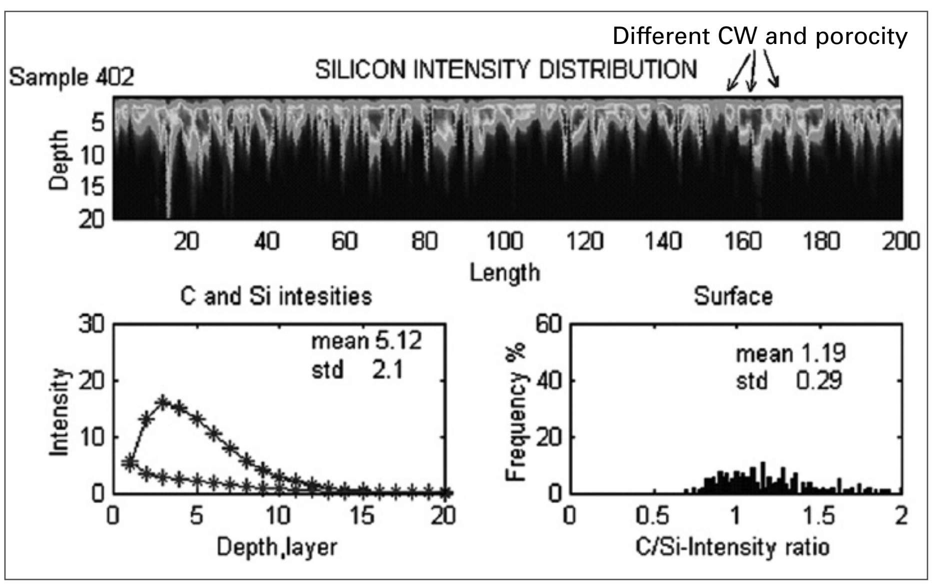

11. Typical coating coverage for LWC with 100% clay, 6% starch and 6% latex, 10 mm deep analysis, measured with LIPS (6). Early consolidation leads to different porosity than late consolidation, if the drying is not alike. Intensity of carbon (binder) in the surface is higher than intensity of Si (clay).

coating (the hills) have already been consolidated in moderate conditions during initial drying. The term "coating solids" used in drying studies is only pointing to average solids of the coating.

CONCLUSIONS

From this study, we reached the following conclusions:

- High web temperature after coating and at the beginning stages of drying increased paper roughness and decreased paper gloss.
- The results obtained with our drying model indicate that water movement into blade-coated LWC base paper is dominated by diffusion when temperature is moderate or high. Capillary flow is restricted to the surface of the base paper.
- When coating color contains latex as the only binder, mottle is caused by uneven coating structure formation in the in-plane direction, probably caused by uneven shrinkage of the adjacent coating.
- Variations in mottle because of drying are large when a coating color contains starch as a water-soluble binder. Uneven binder concentration caused by uneven binder migration increases mottle tendency.
- Layouts of pilot coater drying sections usually restrict the capabilities to investigate the influence of drying. For example, too long a delay before reaching the evaporative drying stage leads to situations where part of the coating is consolidated before proper drying by drainage, which masks the impact of different drying strategies.
- Coating color mass distribution on the surface of LWC paper is often so wide that using the average solids contents of coating color as a variable in drying studies can lead to questionable conclusions. **TJ**

ACKNOWLEDGEMENTS

The authors thank Vaito Laaja for arranging the pilot trials. Pasi Rajala also thanks VTT Energy (Technical Research of Finland) for the opportunity to develop the simulation program and for the excellent working environment. The authors thank Nick Triantafillopoulos of RohmNova, *TAPPI JOURNAL* Technical Editor, for excellent advice and helpful comments.

LITERATURE CITED

1. Watanabe, J., and Lepoutre, P., *J. Applied Polymer Sci.* 27: 4207(1982).
2. Graab, H., *Wochenblatt fur papierfabrikation* (17): 645(1983).
3. Hagen, K., *TAPPI 1985 Coating Conference Proceedings*, TAPPI PRESS, Atlanta, Georgia, USA, p. 131.
4. Norrdahl, P., *TAPPI 1991 Coating Conference Proceedings*, TAPPI PRESS, Atlanta, p. 417.
5. Engström, G., Persson, A., Fineman et al., *TAPPI 1982 Coating Conference Proceedings*, TAPPI PRESS Atlanta, p. 109.
6. Rajala, P., Häkkänen, H., Berg, C.-G., et al., *Drying Tech.* 21(10): 1941(2003).
7. Eklund, D., Norrdahl, P., and Heikkinen, M.-L, *Drying Tech.* 13(4): 919(1995).
8. Häkkänen, H., Houni, J., Kaski, S., et al., *Spectrochim. Acta*, 56B: 737(2001).
9. Nowicki, S., Davis, H., and Scriven, L., *TAPPI 1991 Coating Conference Proceedings*, TAPPI PRESS, Atlanta, p. 337.
10. Engström, G., *TAPPI J.* 77(4): 160(1994)
11. Groves, R., Ruggles, C. and Penson, J., *TAPPI 1993 Coating Conference Proceedings*, TAPPI PRESS, Atlanta, p. 187.
12. Kumano, A., Higuchi, A., Watanabe, et al., *TAPPI 1993 Coating Conference Proceedings*, TAPPI PRESS, Atlanta, p. 1.
13. Takase, K., Miura, H., Tamon, H. et al., *Drying Tech.* 12(6): 1279(1994).
14. Skowronski, J. and Lepoutre, P., *TAPPI J.* 68(11): 98 (1985).
15. Kartovaara, I., *1989 International Mechanical Pulping Conference Proceedings*, Vol. 1, p 25.
16. Farkas, I., and Lampinen, M., *Drying Technology*, 9(4):1019(1991)
17. Karlsson, M., and Paltakari, J., *Drying 92*, Vol. 2, Hemisphere, New York, 1992, p. 913,
18. Heikkilä, P., Ph.D. thesis, Åbo Akademi University, Turku, Finland, 1993.
19. Rajala, P., and Karlsson, M., *1995 IMECE, Proceedings of the ASME Heat Transfer Division*, HTD-Vol. 317-2, p. 445.
20. Åkerholm, J., Berg, C-G., and Kirstilä V., *Drying Tech.* 19(10): 2407(2001).
21. Rajala, P., Koskinen, T., Nieminen, K. et al., *Proceedings of the 10th International Coating Science and Technology Symposium* (ISCST '2000), p. 232.
22. Joronen, H., Master of Science Thesis, Lappeenranta University of Technology, Laboratory of Paper Technology, 1999.

Received: December 8, 2002
Revised: March 26, 2004
Accepted: March 10, 2004

This paper is also published on TAPPI's web site <www.tappi.org> and summarized in the July *Solutions! for People, Processes and Paper* magazine (Vol. 87 No. 7).

INSIGHTS FROM THE AUTHORS

I chose this topic to research because I felt that there were unanswered questions in this field. This research verifies studies made by others and specifies some findings made with longer delay time to drying. At the same time, this study expands to the area of shorter delay time, which has not been studied before.

The most difficult aspect of this research was working to compare different tests made at different pilot machines. The simulation model was very helpful in this regard.

The most surprising thing about these research results was that it was so hard to believe the new findings and to change my own opinion. The old theory was restricting new thinking.

I believe mills can benefit from this information because it can be used to simplify drying sections for LWC machines. The next step would be new pilot machine tests with new drying layouts. These have partly been done already, and the new results verify results made in this study.

— Pasi Rajala

Rajala

Koskinen

Rajala is with Metso Paper, Air Systems, Pansiontie 56, Fin-20240, Turku, Finland. Email Rajala at pasi.rajala@metso.com. Koskinen is with UPM-Kymmene, R&D, P.O. Box 51, 37601 Valkeakoski, Finland. Email Koskinen at timo.m.koskinen@upm-kymmene.com.

APPENDIX A

Major equations used in the model

Darcy law is used to model capillary flow:

$$\rho w = \frac{k_2}{\nu_2}\frac{\partial p_2}{\partial x} \qquad (1)$$

For capillary pressure Kelvin equation is used:

$$p_2 - p_{20} = \frac{1}{\nu_2}\frac{RT}{M_3}\ln(\varphi) \qquad (2)$$

Sorption isotherm equation is according to Karlsson et al. [15]:

$$\varphi(u,T) = 1 - \exp(-mu^n) \qquad (3)$$

For vapor flow Eq. 4 is used [14]:

$$\rho_3 w_3 = -\varepsilon_a \frac{p_\beta}{(p_\beta - p_3)}\frac{M_3}{RT} D_{34}\frac{\partial p_3}{\partial x} \qquad (4)$$

For heat transfer between paper and ambient air Eq. 5 is used:

$$q = \alpha(T_{ms} - T_4) \qquad (5)$$

Mass transfer is modeled as

$$\dot{m} = KM_3 \ln\left(\frac{P_{4,a}}{p_{4,ms}}\right) \qquad (6)$$

Eq. 1 and 4 are combined to model mass flow:

$$\rho_1 \frac{\partial u}{\partial t} = \frac{\partial}{\partial x}\left(\frac{k_2}{\nu_2}\frac{\partial p_2}{\partial x} + \varepsilon_b \frac{M_a}{RT} D_3 \frac{\partial p_3}{\partial x}\right) \qquad (7)$$

Heat flow is combination of convection and conduction:

$$\rho c_p \frac{\partial T}{\partial t} = l \frac{\partial}{\partial x}\left(\varepsilon_b \frac{M_a}{RT} D_v \frac{\partial p_3}{\partial x}\right) + \frac{\partial}{\partial x}\left(\lambda \frac{\partial T}{\partial x}\right) \qquad (8)$$

IR drying is modelled by assuming that energy is absorbed evenly in the thickness direction of paper. Radiation energy absorption in the web is then:

$$r_n = r_0 \eta / (nw) \qquad (9)$$

Symbols used

w	flow velocity	m/s
p	pressure	Pa
x	length coordinate	m
R	gas constant	J/mol K
T	temperature	K
M	molar mass	g/mol
m	constant in isotherm	(-)
u	moisture	kg_{water}/kg_{dry}
n	constant in isotherm	(-)
q	heat flux	W/m^2
m	mass	kg
K	mass transfer coefficient	$kmol/m^2s$
k	water conductivity	m^2
l	latent heat of evaporation	kJ/kg
n	amount of layers in Z-direction	(-)
w	width of the machine	m
r	radiation energy	kW

Greek letters

α	convective heat transfer coefficient	W/m^2K
ε	diffusion resistance coefficient	(-)
λ	heat conductivity	W/mK
φ	relative vapor pressure	(-)
η	efficiency (part of energy absorbed)	(-)
ρ	partial density	kg/m^3
ν	kinematics visciosity	m^2/s

Indexes

2	water
3	vapor
4	air
c	coating
a	drying air
ms	moist solid phase
ev	evaporation
β	moist air